ACS APPLIED ENERGY MATERIALS

www.acsaem.org Article

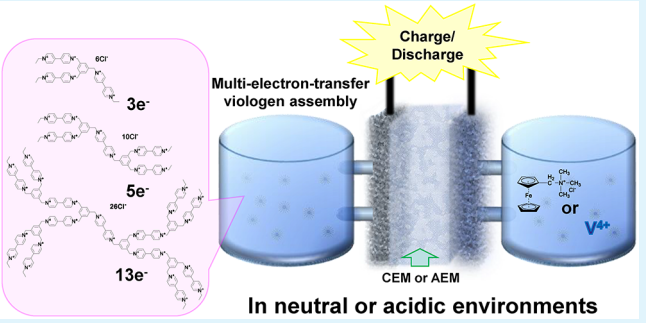
Redox-Flow Battery Operating in Neutral and Acidic Environments with Multielectron-Transfer-Type Viologen Molecular Assembly

Akihiro Ohira,* Takashi Funaki,* Erika Ishida, Je-Deok Kim, and Yukari Sato

Cite This: https://dx.doi.org/10.1021/acsaem.0c00067 Read Online

ACCESS | Metrics & More | Article Recommendations | Supporting Information

ABSTRACT: Recently, redox flow batteries (RFBs) have attracted attention as a large-scale energy storage technology. To improve their energy density, we investigated organic-based active materials with high water solubility, synthesized regular dendritic structures comprising viologen molecular assemblies, and applied them to RFBs. The compounds containing 3, 5, and 13 viologen molecular units showed electrolysis activity corresponding to the number of units, and it was found that the redox reaction progressed quantitatively. Furthermore, the charge and discharge characteristics confirmed that the energy efficiency was improved compared to methyl viologen batteries. These compounds have high solubility, and the viologen derivatives can function in acidic conditions, in which methyl viologen does not work as a redox active material, due to reduced interaction between molecules and the cation exchange membrane. Finally, molecules having 5 and 13 viologen units can be prepared to concentrations of 1 and 0.5 M, theoretically reaching a capacity of 134 and 174 Ah/L, respectively.



KEYWORDS: *redox flow battery, organic molecules, aqueous solution, molecular assembly, dendritic structure, viologen*

Downloaded via NATL INST ADVNCD IND SCI & TECHLGY on April 29, 2020 at 23:45:27 (UTC).
See https://pubs.acs.org/sharingguidelines for options on how to legitimately share published articles.

INTRODUCTION

The introduction of power generation systems using natural energy, such as solar and wind power, into power grids is being promoted in various countries around the world. Although they do not generate greenhouse gases, such as carbon dioxide, compared to power sources like thermal and hydroelectric power, these renewable energy sources provide an unstable power supply that is affected by various conditions, such as location and climate. To use renewable energy efficiently, the generated electricity must be stored and discharged as needed; thus, a storage battery (secondary battery) that can adjust the constantly fluctuating output over short and long cycles is greatly needed.

Large-capacity storage batteries include lithium-ion batteries, sodium−sulfur batteries, lead-acid batteries, and redox flow batteries (RFBs),[1−3] and these storage batteries have been used for distributed power systems in various places depending on the size and application. Above all, although RFBs[4,5] have technical issues, including energy density lower than that of other storage batteries, and their vanadium content makes them expensive, they have long life and high design flexibility. In addition, they operate at normal temperature and pose no danger of thermal runaway or explosion. Therefore, the advantages of RFBs have been attracting attention as one way to achieve power leveling for renewable energy.

RFBs were successfully developed by NASA around 1974.[6] At the beginning of development, the Fe/Cr system was the leading technology,[7] but it was not put into practical use because mixing of the positive and negative electrolytes through the membrane decreases the capacity of the battery. Around 1984, Skyllas-Kazacos et al. developed a vanadium-based RFB,[8] and since that time, the awareness of RFBs has increased and research and development has been accelerating.

A RFB mainly comprises an electrode, an electrolyte membrane, and an electrolyte. A carbon felt or carbon paper is used as the electrode, and to improve the reactivity with the electrolytic solution, metal particles can be incorporated into the carbon as a catalyst. The electrolyte membrane prevents mixing of the active materials of the positive and negative electrodes, and it is responsible for the ion transport and charge compensation associated with charge and discharge. Vanadium RFBs mainly use a proton-conducting membrane, such as Nafion. In recent years, materials research on electrolyte membranes, electrodes, and diffusion layers, which were cultivated during research and development of polymer electrolyte fuel cells, has improved cell design technology and battery performance.[9]

Received: January 12, 2020
Accepted: April 16, 2020
Published: April 16, 2020

© XXXX American Chemical Society

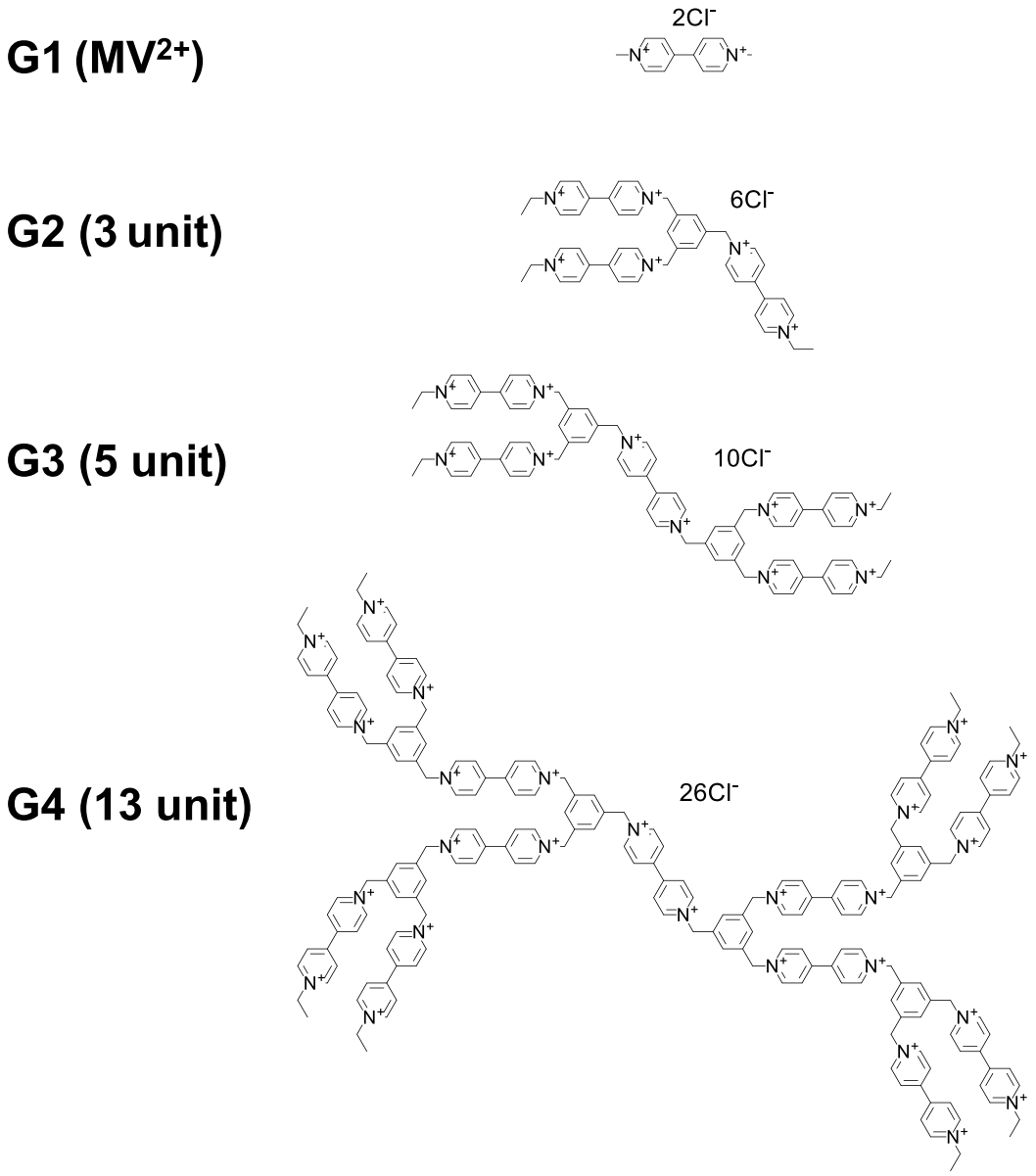


Figure 1. Chemical structures of four generations of viologen molecular assemblies.

More recently, research on alternative technology, such as organic, Ti−Mn,[10] or hybrid RFBs,[11−13] has become active, and in terms of performance, some alternative RFBs, especially organic RFBs, have become comparable to high-cost vanadium RFBs. One of the greatest features of organic RFBs is that it is possible to increase the energy density by controlling the solubility and redox potential based on molecular design, and pioneering and unique research has been reported so far.[14−20] The electron transfer reaction rate of the active material in an organic RFB is larger than that in a vanadium RFB, and the reactivity with the carbon electrode is relatively good. For this reason, continued development of RFBs is expected to provide a new power storage technology that can flexibly cope with being combined with other secondary batteries and hydrogen production technologies.

Viologen and its derivatives have been widely studied as model compounds for photoelectrochemistry,[21−25] and in recent years have also been studied as organic active materials in RFBs.[25−32] Promising characteristics of viologen compounds for RFBs include that they can be applied to both aqueous and nonaqueous systems by means of counterion species, have relatively high solubility, and have high redox stability. Janoschka et al. designed an active material group in which viologen molecules are introduced into a polymer backbone, and they reported the possibility of improved energy density.[26] Beh et al. designed highly water-soluble viologen and ferrocene derivatives as anolytes and catholytes, respectively, for aqueous RFBs. They also reported that organic RFBs show excellent charge−discharge cycling performance comparable to that of vanadium RFBs.[27] Another study reported that charge and discharge cycles are stabilized by changing the functional group bonded to the viologen molecule.[28] Burgess et al. synthesized a double-headed molecule containing a viologen unit and discussed the effect of the backbone structure on the electrochemical performance.[33]

Currently, we are focusing on viologen units and have newly synthesized an assemblage of viologen molecules with relatively high symmetry and a regular structure. A regular

https://dx.doi.org/10.1021/acsaem.0c00067
ACS Appl. Energy Mater. XXXX, XXX, XXX−XXX

structure, such as a highly symmetrical dendrimer, can increase the solubility and viscosity of a solution, accompanied by an increase in molecular weight.[34] We are adopting that concept for active material design and aim at improving RFB performance by increasing both the solubility of the designed viologen assembly and the redox response of the individual introduced viologen molecules. Here, we report the application of this idea to aqueous RFBs using newly synthesized viologen molecular units for an anolyte with a relatively high symmetry and regular structure.

Here, we report the use of methyl viologen (MV^{2+}) as the first generation (G1) and synthesis of compounds to which 3 (G2), 5 (G3), and 13 (G4) viologen molecular units were bound (Figure 1). These compounds, which have a chloride counterion and relatively high water solubility, were used for electrochemical measurements and charge−discharge tests.

The solubility of those compounds in 1 M NaCl aqueous solution is 0.5 M for G2, 1 M for G3, and 0.5 M for G4. In the cases of G3 and G4, solubilities of 1 and 0.5 M are equivalent to 5 and 6.5 M when converted to per-viologen-unit values, respectively, and those values correspond to theoretical capacities of 134 and 174 Wh/L as dication states per unit, respectively. These results clearly indicate that viologen units do not aggregate when they are assembled in a regular framework with relatively high symmetry, which suppresses the decrease of molecular solubility.

ELECTROCHEMICAL PROPERTIES OF VIOLOGEN DERIVATIVES

Cyclic voltammetry using a glassy carbon electrode as the working electrode revealed two peaks on each of the oxidation and reduction sides of each sample. The peak on the positive side indicates a one-electron redox reaction, and the peak on the negative side indicates a two-electron redox reaction (Figure S13). As the two-electron reaction progresses, the glassy carbon surface developed a film-like appearance. This indicates that the loss of charge desorbed Cl^- counterions, resulting in a decrease in solubility and aggregation on the electrode surface.

Table 1 shows the viscosity of the solutions having relatively low and high concentrations of G1, G2, G3, and G4 in D_2O, and the cell resistance of the sample solutions prepared so that the viologen unit was equivalent to 0.1 M. Since the cell resistance is the same for the type of the carbon electrode and the membrane used, these comparisons reflect the resistance of the sample solution.

Table 1. Viscosity and Cell Resistance of G1, G2, G3, and G4 Solution[a]

	G1	G2	G3	G4
viscosity at 0.5 M (mPa·s)	1.6	2.1	2.3	3.0
viscosity at 2.0 M	6.3		34	28
cell resistance ($\Omega \cdot cm^2$) at 0.1 M	1.5	1.5	2.8	2.5

[a]The sample concentrations shown here are equivalent to viologen units. 2 M equivalent of G2 cannot be prepared due to low solubility.

At relatively low concentrations (0.5 M), the increase in viscosity of G3 and G4 is small relative to the increase in molecular weight, even when compared to G1. At higher concentrations, the increase in viscosity tends to be greater than at lower concentrations, but interestingly, there is no significant difference in viscosity between G3 and G4. This indicates that the introduction of the dendritic-type regular structure might be effective in controlling the viscosity of the electrolyte, which is one of the causes of loss of system efficiency in the flow battery.

To conduct electrochemical measurements closer to RFB operating conditions, a carbon felt (diameter 0.5 cm) and electrolyte membrane (Selemion DSV or Nafion NR212) were placed in a small test cell, and the redox property of active materials as catholytes and anolytes was evaluated (Figure S15). Figure 2 shows the current potential curves of the four synthesized viologen molecular assemblies. The value of $E_{1/2}$ is around −0.64 V (vs Ag/AgCl) for G1, whereas G2, having 3 viologen units, is around −0.49 V and G3, having 5 units, is around −0.47 V. Moreover, G4, with 13 units, is shifted to the noble potential side, around −0.44 V. Because the viologen unit in the framework has an ethyl group and a benzyl group bonded together, the redox potential is thought to have shifted to the positive side compared to G1.

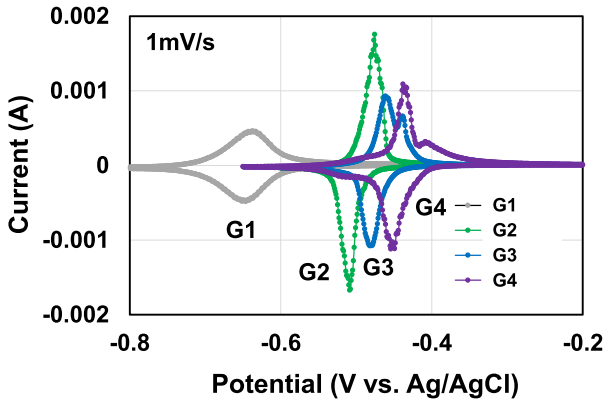


Figure 2. Current−potential (I−E) curves of viologen molecular assemblies. Scan rate: 1 mV/s. Concentration of active material: 10 mM G1, 3.5 mM G2, 2 mM G3, and 0.77 mM G4. Supporting electrolyte: 1 M NaCl. Counter electrode: Carbon felt (AAF304ZS). Reference electrode: Ag/AgCl.

The amount of charge from the current−potential curve in Figure 2 was estimated to obtain the number of reaction electrons from the ratio of the actual amount of electrolysis and the active material concentration present in the electrode (Figure S16). As a result, the ratio of the actual reactant and active material concentration in the electrode was 0.98 for G1, 2.8 for G2, 4.1 for G3, and 14 for G4. If one electron is involved in the redox reaction in each unit, almost all of the introduced viologen units contributed to the one-electron redox reaction. These results indicate that a multielectron reaction system corresponding to the number of introduced molecules can be realized.

The absorption coefficients obtained from the UV−vis absorption spectra of the G3 and G4 aqueous solutions (Figure S17) are 21 100 M^{-1} cm^{-1} and 20 900 M^{-1} cm^{-1} when converted to (viologen) unit equivalents. These values are close to those reported for MV^{2+}.[35] This indicates that the viologen unit introduced into the molecular assembly does not aggregate within the framework, and each behaves in isolation, and this also supports the results that all of the introduced viologens can contribute to the redox reaction.

Heinen et al. reported a spectroelectrochemical analysis of reaction mechanisms in a dendrimer structure linked with a viologen unit.[36,37] They synthesized nonaqueous compounds

https://dx.doi.org/10.1021/acsaem.0c00067
ACS Appl. Energy Mater. XXXX, XXX, XXX−XXX

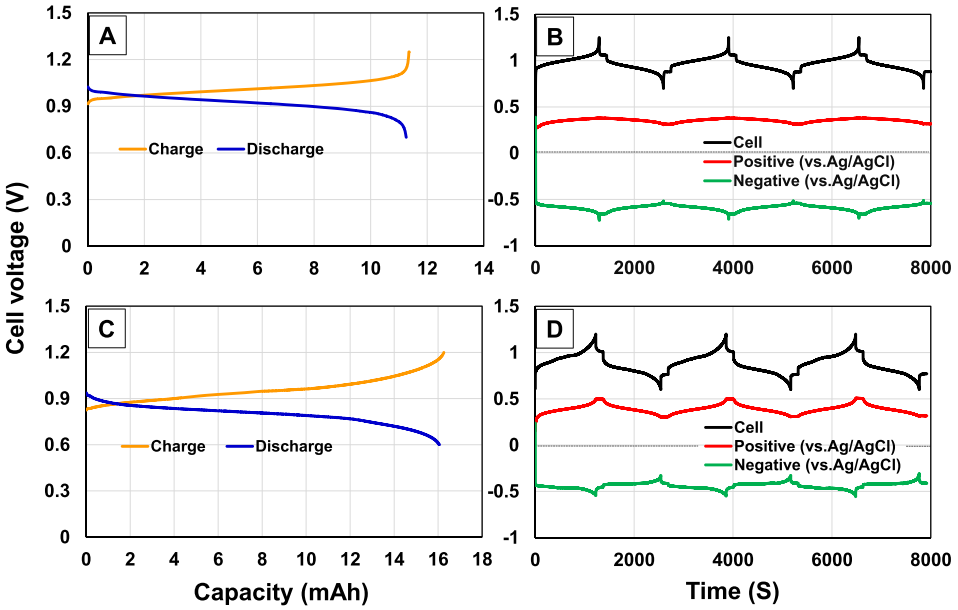


Figure 3. Galvanostatic charge−discharge performance of Fe-TMACl−G1 flow battery (A, B) and Fe-TMACl−G3 flow battery (C, D) in neutral media. (A, C) Relationship between cell voltage and capacity in second cycle. (B, D) Change in cell voltage and positive and negative electrode potential vs Ag/AgCl in three charge−discharge cycles. The current efficiency, voltage efficiency, and the energy density were estimated from the charge−discharge curve of the second cycle. Applied current density: 10 mA/cm^2. Concentration: (A) 0.15 M Fe-TMACl−0.1 M G1 in 1 M NaCl, (C) 0.1 M Fe-TMACl−0.04 M G3 in H_2O. Volume of electrolyte solution: (A) positive 10 mL, negative 5 mL, (C) positive 7 mL, negative 7 mL. Flow rate (A, B): 20 mL/min. Membrane: Selemion DSV. Electrode: AAF304ZS (active area of 5 cm^2).

with a PF_6^- counterion, which have a structure similar to our G2, G3, and G4 molecular structures. According to their report, G3 and G4 had a fast reduction reaction, and the oxidation reaction occurs in stages in the core phenyl and outer benzyl viologen (BV^{2+}) units. In the G3 and G4 current−voltage measurements in Figure 2, the reduction reaction is a single peak, whereas the oxidation reaction is split, as reported by Heinen et al.[37] Similar to nonaqueous systems, the reaction rate in an aqueous solution system would also be different between the reduction and oxidation side.

Interestingly, G2, G3, and G4 were found to show reversible redox reactions even in acidic solutions with Nafion as the electrolyte membrane (Figure S18). In the case of G1, only a reduction reaction was observed. To investigate the cause of the difference in redox behavior in acidic solutions, a crossover test between G1 and G2 was performed using Nafion. The mobility of G1 and G2 between acidic solutions at the same concentration on both sides of the Nafion membrane was compared. There was a tendency for MV^{2+} to move to the opposite side over time compared to G2 (Figure S19). In contrast, in the case of G2, it was found that movement to the sulfuric acid solution on the opposite side seemed to be suppressed.

When Nafion is hydrated, the cluster structure in which perfluorosulfonic acid groups in Nafion are assembled becomes larger due to the inclusion of water molecules, and the water channel structure is 3.6 nm in diameter from the small-angle X-ray scattering measurements (Figure S20), which is consistent with previously reported results.[38] When the diffusion coefficient was estimated from the Levich plot obtained from hydrodynamic voltammetry (Figure S21), the diffusion coefficient tended to decrease as the number of molecules increased. In addition, there is a linear relationship between the number of units and the diffusion coefficient, indicating that the introduced molecules do not aggregate but rather enter the framework in an orderly manner (Figure S22). The hydrodynamic radius calculated by Stokes−Einstein equation from the diffusion coefficient was 1.16 nm for G2, 1.42 nm for G3, and 2.72 nm for G4. Although the molecular size of G2 is smaller than 3.6 nm (1.8 nm radius), when considered as the size of the hydration structure including counterions, it might be difficult for G2 with high symmetry to diffuse through the 4 nm channel in Nafion. In contrast, MV^{2+} has a smaller molecular size than G2 and is likely to diffuse in the channel, so a stable redox reaction on the electrode surface is not expected. In fact, reversible one-electron redox reactions of MV^{2+} were observed by ordinary three-electrode cyclic voltammetry in acidic solutions using a glassy carbon electrode (Figure S14). Therefore, it is thought that these differences in redox behavior are caused by diffusion of molecules through the Nafion membrane. For details, structural and electronic state analysis, including the hydration structure, is necessary.

CHARGE−DISCHARGE CHARACTERISTICS IN NEUTRAL CONDITION

Figure 3 compares the charge and discharge characteristics when the catholyte was ferrocene trimethylammonium chloride (Fe-TMACl) dissolved in NaCl aqueous solution and the anolyte was G1 (Figure 3A,B) and G3 (Figure 3C,D) dissolved in 1 M NaCl aqueous solution. Selemion-DSV was used for the anion exchange membrane. For G1, when the catholyte concentration was 0.15 M and the anolyte was 0.1 M, the Coulomb efficiency and the voltage efficiency were 99% and 91%, respectively. The energy density was 0.69 Wh/L. In contrast, for G3, when the catholyte and anolyte concentrations were 0.1 and 0.04 M, the Coulomb efficiency and voltage efficiency were 99% and 83%, respectively, and the energy density was 0.91 Wh/L. Compared with G1, G3 has a higher energy density despite the lower active material

https://dx.doi.org/10.1021/acsaem.0c00067
ACS Appl. Energy Mater. XXXX, XXX, XXX−XXX

concentration, again indicating that each intramolecular unit contributes to the redox reaction.

We have estimated the utilization of the theoretical capacity for each generation: G1 is 84%; G3 is 43%. The origin of these low utilization might be due to local inhomogeneity of intramolecular or intermolecular reactions in flow battery system. Although the electrochemical measurement allows a multielectron-transfer reaction by one-electron reaction of each viologen unit, these results clearly show that there is room for further improvement from the viewpoint of application as a flow battery.

When the catholyte concentration was increased to 1 M and the anolyte concentration with G3 was increased to 0.2 M, the Coulomb efficiency and voltage efficiency were 98% and 76%, respectively, and the energy density was 7.8 Wh/L (Figure S23).

The anolyte was dissolved by about 1 M in the case of G3 in an uncharged state, that is, when the charge state in the unit was a dication. This is a concentration corresponding to about 5 M in MV^{2+}. However, in the cation radical state generated by the one-electron reduction reaction, the counterions are decreased as compared with the dication, which likely lowers the solubility. It is emphasized here that such a molecular assembly has a higher solubility than MV^{2+}, and it can be a candidate structure that potentially contributes to an improvement in energy density, provided that a suitable catholyte is also designed.

The cycle test at high concentration, which is the one of the most important index of the performance for the flow battery, was also performed as shown in Figure 4 (catholyte, 1 M Fe-TMACl in 1 M NaCl; anolyte, 77 mM G4 in 1 M NaCl). We have found that the capacity drastically decreased after 10 cycles. When the cell after the test was disassembled, the surface of the membrane which was in contact with the positive electrode was discolored and some precipitation was also observed. The results of FT-IR and UV−vis measurement (Figures S24 and S25) revealed that the precipitation was derived from Fe-TMACl. In addition, Fe-TMACl adsorbed inside the membrane cannot be removed by washing. This phenomenon was also reproduced in the flow battery test at relatively low concentrations (Figure S26), suggesting that strong interaction existed between the membrane interface and Fe-TMACl. Although Liu et al. have achieved high-cycling stability with the Fe-TMACl and MV^{2+} flow battery system,[30] the membranes they used differed from our experimental systems, so further optimization is needed in our cases.

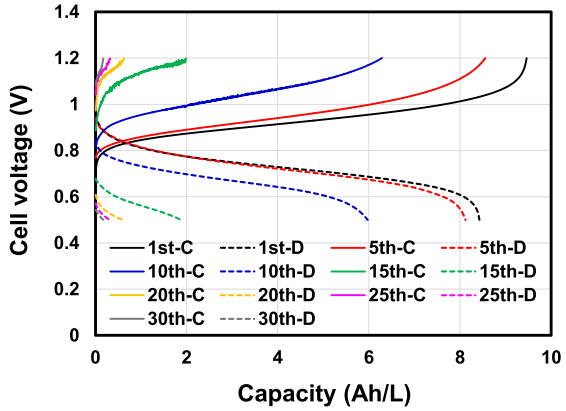


Figure 4. Charge−discharge profiles of selected cycles of Fe-TMACl−G4 battery at 13 mA/cm^2. Concentration: 1 M Fe-TMACl in 1 M NaCl aq and 0.077 M G4 in 1 M NaCl aq. Due to extremely low capacity, the data after 30 cycles were omitted.

For the anolyte, CV measurement of G4 before and after cycling test was performed to confirm whether there was any change. As a result, a decrease in the redox current and a peak shift have been observed (Figure S27). This suggests that some of the viologen units may have changed during the cycling. Since the CV profile is similar, it is considered that the molecular framework might be still maintained.

Although in the electrochemical measurement without flow, those materials that can perform a multielectron-transfer reaction due to a one-electron reduction reaction, in a battery test, the reaction distribution is highly likely to occur, and a two-electron reduction reaction may be induced during the cycling test. As a result, side reactions such as dimerization between molecules might happen resulting in structural change. Therefore, the main possible causes of the capacity decrease are assumed as follows:

(1) Overvoltage rise due to adsorption of positive electrode active material on membrane surface and inside.

(2) Partial insolubilization of viologen unit by progress of partial two-electron reduction.

CHARGE−DISCHARGE CHARACTERISTICS IN ACIDIC CONDITION

Basically, viologen cannot function as a flow battery in acidic environment using Nafion. This is because the sulfonic acid group of Nafion strongly interacts with viologen, and in order to avoid this strong interaction, a molecule containing the same sulfonic acid group as the side chain functional group of Nafion must be introduced into the viologen skeleton.[32] We previously discussed how the viologen molecular assembly shows a reversible redox reaction in acid using Nafion proton exchange membrane. This indicates that charging and discharging are possible using an acidic electrolyte and a proton exchange membrane.

Figure 5A,B shows the results of a charge−discharge test with a Nafion electrolyte membrane, aqueous vanadium oxide sulfate as the catholyte, and G3 aqueous solution as the anolyte. For comparison, a charge−discharge test was also conducted using a sulfuric acid aqueous solution of BV^{2+} as the anolyte (Figure 5C,D). When a molecule has a viologen unit, the redox reaction does not depend on pH, unlike redox with a quinone molecule. Therefore, a molecule having a positive redox potential can be selected for the catholyte, as compared with the neutral solution, to improve the energy density.

In fact, the energy density of the acidic solution was higher than that of the neutral solution. In G2, the Coulombic efficiency and voltage efficiency were 93% and 86%, respectively, and the energy density was 1.12 Wh/L. In G3, the Coulombic efficiency and voltage efficiency were 91% and 90%, respectively, and the energy density is 1.07 Wh/L, which is higher than that for the neutral solution. This is because the electromotive force is increased by using vanadium as the catholyte. For G4, the viologen unit equivalent concentration was about half of that of G2 and G3; the Coulomb efficiency and voltage efficiency were 94% and 81%, respectively; and the energy density was 0.42 Wh/L. For comparison, the energy density of a 0.5 M BV^{2+}−0.5 M $VOSO_4$−1.5 M H_2SO_4 flow battery was 0.22 Wh/L, which is lower than those of G2, G3,

https://dx.doi.org/10.1021/acsaem.0c00067
ACS Appl. Energy Mater. XXXX, XXX, XXX−XXX

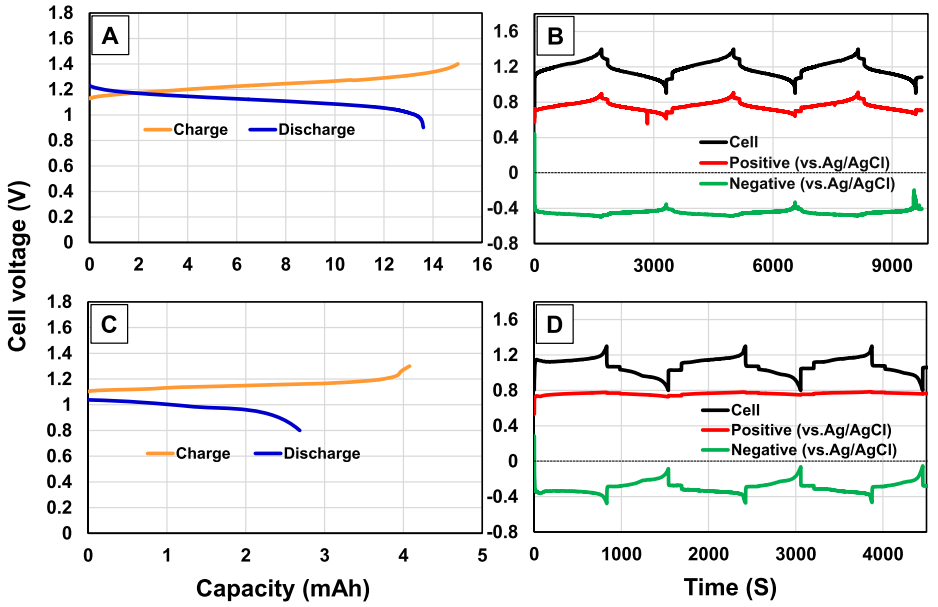


Figure 5. Galvanostatic charge−discharge performance of vanadium−G3 flow battery (A, B) and vanadium−BV^{2+} flow battery (C, D) in acidic media. (A, C) Relationship between cell voltage and capacity in second cycle. (B, D) Change in cell voltage and positive and negative electrode potential vs Ag/AgCl in three charge−discharge cycles. The current efficiency, voltage efficiency, and the energy density were estimated from the charge−discharge curve of the second cycle. Applied current density: 7 mA/cm^2. Concentration: (A) 0.1 M $VOSO_4$ in 0.3 M H_2SO_4−0.1 M G3 in H_2O, (B) 0.5 M $VOSO_4$ in 1.5 M H_2SO_4−0.5 M BV^{2+} in 1.5 M H_2SO_4. Volume of electrolyte solution: (A) positive 7 mL, negative 7 mL, (C) positive 6 mL, negative 6 mL. Flow rate: (A) 20 mL/min, (C) 3 mL/min. Membrane: Nafion NR212. Electrode: AAF304ZS (active area of 5 cm^2).

and G4, despite the relatively high acid concentration. In addition, the Coulomb efficiency is as low as about 66%, and interaction with the Nafion membrane is thought to reduce reactivity with the electrode. It is emphasized here that our molecules can be operated in acidic conditions where MV^{2+} does not work, and the origin is control of the interaction between the membrane surfaces and molecules by adjusting the molecular size. Thus, the cation exchange membrane other than Nafion can be used to operate the RFB in the neutral region. This has the advantage of increasing the choice of active materials on the positive electrode side.

CONCLUSION

We applied a newly designed viologen-assembled regular structure as an anolyte to create a high-performance RFB.

Here, by introducing a dendrimer-type molecular structure, we succeeded in developing a highly water-soluble active material and demonstrated that we can operate as a flow battery in both neutral and acidic environments. However, significant issue with cycling stability has also been found, and further study will be needed to search for a more stable structure that would not cause side reactions such as dimerization.

Currently, we have developed only the anolyte, but our concept can also be applied to the catholyte. Because radical-based redox reactions with viologen derivatives do not depend on pH, these materials are promising for improving RFB energy density.

ASSOCIATED CONTENT

Supporting Information

The Supporting Information is available free of charge at https://pubs.acs.org/doi/10.1021/acsaem.0c00067.

Synthesis details, NMR spectra, and additional experimental details (PDF)

AUTHOR INFORMATION

Corresponding Authors

Akihiro Ohira − *Research Institute for Energy Conservation, National Institute of Advanced Industrial Science and Technology (AIST), Tsukuba, Ibaraki 305-8565, Japan*; orcid.org/0000-0002-5748-4830; Email: a-oohira@aist.go.jp

Takashi Funaki − *Research Center for Photovoltaics, AIST Tsukuba Central 5, Tsukuba, Ibaraki 305-8565, Japan*; Email: takasi-funaki@aist.go.jp

Authors

Erika Ishida − *Research Institute for Energy Conservation, National Institute of Advanced Industrial Science and Technology (AIST), Tsukuba, Ibaraki 305-8565, Japan*

Je-Deok Kim − *Hydrogen Production Materials Group, Center for Green Research on Energy and Environmental Materials, National Institute for Materials Science, Tsukuba, Ibaraki 305-0044, Japan*

Yukari Sato − *Research Institute for Energy Conservation, National Institute of Advanced Industrial Science and Technology (AIST), Tsukuba, Ibaraki 305-8565, Japan*

Complete contact information is available at: https://pubs.acs.org/10.1021/acsaem.0c00067

Notes

The authors declare no competing financial interest.

ACKNOWLEDGMENTS

A.O and T.F. thank Department of Energy and Environment of AIST for funding support of seeds research. The small-angle X-ray scattering (SAXS) was measured by using the beam time allotted from Proposal 2017G687 at Photon Factory of KEK. The authors thank Hideaki Takagi and Nobutaka Shimizu of KEK-PF for their help with the SAXS measurements.

https://dx.doi.org/10.1021/acsaem.0c00067
ACS Appl. Energy Mater. XXXX, XXX, XXX−XXX

REFERENCES

(1) Zakeri, B.; Syri, S. Electrical energy storage systems: A comparative life cycle cost analysis. *Renewable Sustainable Energy Rev.* **2015**, *42* (2015), 569−596.

(2) Shi, F. *Reactor and Process Design in Sustainable Energy Technology*; Elsevier: Amsterdam, 2016.

(3) Dunn, B.; Kamath, H.; Tarascon, J.-M. Electrical Energy Storage for the Grid: A Battery of Choices. *Science* **2011**, *334*, 928−935.

(4) Noack, J.; Roznyatovskaya, N.; Herr, T.; Fischer, P. The Chemistry of Redox-Flow Batteries. *Angew. Chem., Int. Ed.* **2015**, *54*, 9776−9809.

(5) Soloveichik, G. L. Flow Batteries: Current Status and Trends. *Chem. Rev.* **2015**, *115*, 11533−11558.

(6) Theller, L. H. *Electrically Rechargeable Redox Flow Cells*; NASA TM X-71540; National Aeronautics and Space Administration: Washington, DC, 1974; pp 1−5.

(7) Gahn, R. F.; Hagedorn, N. Negative-Electrode Catalysts for Fe/Cr Redox Cells. *NASA Tech Briefs*; NASA, February 1987; pp 42−43.

(8) Skyllas-Kazacos, M. S.; Rychcik, M.; Robins, R. G.; Fane, A. G.; Green, M. A. New All-Vanadium Redox Flow Cell. *J. Electrochem. Soc.* **1986**, *133*, 1057−1058.

(9) Dennison, C. R.; Agar, E.; Akuzum, B.; Kumbur, E. C. Enhancing Mass Transport in Redox Flow Batteries by Tailoring Flow Field and Electrode Design. *J. Electrochem. Soc.* **2016**, *163*, A5163−A5169.

(10) Dong, Y. R.; Kaku, H.; Hanafusa, K.; Moriuchi, K.; Shigematsu, T. A Novel Titanium/Manganese Redox Flow Battery. *ECS Trans.* **2015**, *69*, 59−67.

(11) Xu, Y.; Wen, Y.; Cheng, J.; Cao, G.; Yang, Y. Study on a single flow acid Cd−chloranil battery. *Electrochem. Commun.* **2009**, *11*, 1422−1424.

(12) Wei, X.; Xu, W.; Vijayakumar, M.; Cosimbescu, L.; Liu, T.; Sprenkle, V.; Wang, W. TEMPO-Based Catholyte for High-Energy Density Nonaqueous Redox Flow Batteries. *Adv. Mater.* **2014**, *26*, 7649−7653.

(13) Huskinson, B.; Marshak, M. P.; Suh, C.; Er, S.; Gerhardt, M. R.; Galvin, C. J.; Chen, X.; Aspuru-Guzik, A.; Gordon, R. G.; Aziz, M. J. A metal-free organic−inorganic aqueous flow battery. *Nature* **2014**, *505*, 195−198.

(14) Yang, B.; Hoober-Burkhardt, L.; Wang, F.; Prakash, G. K. S.; Narayanan, S. R. An Inexpensive Aqueous Flow Battery for Large-Scale Electrical Energy Storage Based on Water-Soluble Organic Redox Couples. *J. Electrochem. Soc.* **2014**, *161*, A1371−A1380.

(15) Winsberg, J.; Stolze, C.; Muench, S.; Liedl, F.; Hager, M. D.; Schubert, U. S. TEMPO/Phenazine Combi-Molecule: A Redox-Active Material for Symmetric Aqueous Redox-Flow Batteries. *ACS Energy Lett.* **2016**, *1*, 976−980.

(16) Lin, K.; Gómez-Bombarelli, R.; Beh, E. S.; Tong, L.; Chen, Q.; Valle, A.; Aspuru-Guzik, A.; Aziz, M. J.; Gordon, R. G. A redox-flow battery with an alloxazine-based organic electrolyte. *Nat. Energy* **2016**, *1*, 16102.

(17) Hollas, A.; Wei, X.; Murugesan, V.; Nie, Z.; Li, B.; Reed, D.; Liu, J.; Sprenkle, V.; Wang, W. A biomimetic high-capacity phenazine-based anolyte for aqueous organic redox flow batteries. *Nat. Energy* **2018**, *3*, 508−514.

(18) Wang, C.; Yang, Z.; Wang, Y.; Zhao, P.; Yan, W.; Zhu, G.; Ma, L.; Yu, B.; Wang, L.; Li, G.; Liu, J.; Jin, Z. High-Performance Alkaline Organic Redox Flow Batteries Based on 2-Hydroxy-3-carboxy-1,4-naphthoquinone. *ACS Energy Lett.* **2018**, *3*, 2404−2409.

(19) Wang, C.; Li, X.; Yu, B.; Wang, Y.; Yang, Z.; Wang, H.; Lin, H.; Ma, J.; Li, G.; Jin, Z. Molecular Design of Fused-Ring Phenazine Derivatives for Long-Cycling Alkaline Redox Flow Batteries. *ACS Energy Lett.* **2020**, *5*, 411−417.

(20) Yan, W.; Wang, C.; Tian, J.; Zhu, G.; Ma, L.; Wang, Y.; Chen, R.; Hu, Y.; Wang, L.; Chen, T.; Ma, J.; Jin, Z. All-polymer particulate slurry batteries. *Nat. Commun.* **2019**, *10*, 2513.

(21) Ebbesen, T. W.; Ferraudi, G. Photochemistry of Methyl Viologen in Aqueous and Methanolic Solutions. *J. Phys. Chem.* **1983**, *87*, 3717−3721.

(22) Nanasawa, M.; Matsukawa, Y.; Jin, J. J.; Haramoto, Y. Redox photochromism of viologen in organized solid state. *J. Photochem. Photobiol., A* **1997**, *109*, 35−38.

(23) Bird, C. L.; Kuhn, A. T. Electrochemistry of the viologens. *Chem. Soc. Rev.* **1981**, *10*, 49−82.

(24) Striepe, L.; Baumgartner, T. Viologens and Their Application as Functional Materials. *Chem. - Eur. J.* **2017**, *23*, 16924−16940.

(25) Ding, J.; Zheng, C.; Wang, L.; Lu, C.; Zhang, B.; Chen, Y.; Li, M.; Zhai, G.; Zhuang, X. Viologen-inspired functional materials: synthetic strategies and applications. *J. Mater. Chem. A* **2019**, *7*, 23337−23360.

(26) Janoschka, T.; Martin, N.; Martin, U.; Friebe, C.; Morgenstern, S.; Hiller, H.; Hager, M. D.; Schubert, U. S. An aqueous, polymer-based redox-flow battery using non-corrosive, safe, and low-cost materials. *Nature* **2015**, *527*, 78−81.

(27) Beh, E. S.; De Porcellinis, D.; Gracia, R. L.; Xia, K. T.; Gordon, R. G.; Aziz, M. J. A Neutral pH Aqueous Organic−Organometallic Redox Flow Battery with Extremely High Capacity Retention. *ACS Energy Lett.* **2017**, *2*, 639−644.

(28) Hu, B.; Tang, Y.; Luo, J.; Grove, G.; Guo, Y.; Liu, T. L. Improved radical stability of viologen anolytes in aqueous organic redox flow batteries. *Chem. Commun.* **2018**, *54*, 6871−6874.

(29) Hagemann, T.; Winsberg, J.; Grube, M.; Nischang, I.; Janoschka, T.; Martin, N.; Hager, M. D.; Schubert, U. S. An aqueous all-organic redox-flow battery employing a (2,2,6,6-tetramethylpiperidin-1-yl)oxyl-containing polymer as catholyte and dimethyl viologen dichloride as anolyte. *J. Power Sources* **2018**, *378*, 546−554.

(30) Hu, B.; DeBruler, C.; Rhodes, Z.; Liu, T. L. Long-Cycling Aqueous Organic Redox Flow Battery (AORFB) toward Sustainable and Safe Energy Storage. *J. Am. Chem. Soc.* **2017**, *139*, 1207−1214.

(31) Luo, J.; Hu, B.; Debruler, C.; Liu, T. L. A π-Conjugation Extended Viologen as a Two-Electron Storage Anolyte for Total Organic Aqueous Redox Flow Batteries. *Angew. Chem., Int. Ed.* **2018**, *57*, 231−235.

(32) DeBruler, C.; Hu, B.; Moss, J.; Luo, J.; Liu, T. L. A Sulfonate-Functionalized Viologen Enabling Neutral Cation Exchange, Aqueous Organic Redox Flow Batteries toward Renewable Energy Storage. *ACS Energy Lett.* **2018**, *3*, 663−668.

(33) Burgess, M.; Chénard, E.; Hernández-Burgos, K.; Nagarjuna, G.; Assary, R. S.; Hui, J.; Moore, J. S.; Rodríguez-López, J. Impact of Backbone Tether Length and Structure on the Electrochemical Performance of Viologen Redox Active Polymers. *Chem. Mater.* **2016**, *28*, 7362−7374.

(34) Dong, R.; Zhou, Y.; Zhu, X. Supramolecular Dendritic Polymers: From Synthesis to Applications. *Acc. Chem. Res.* **2014**, *47*, 2006−2016.

(35) Watanabe, T.; Honda, K. Measurement of the Extinction Coefficient of the Methyl Viologen Cation Radical and the Efficiency of Its Formation by Semiconductor Photocatalysis. *J. Phys. Chem.* **1982**, *86*, 2617−2619.

(36) Heinen, S.; Walder, L. Generation-Dependent Intramolecular CT Complexation in a Dendrimer Electron Sponge Consisting of a Viologen Skeleton. *Angew. Chem., Int. Ed.* **2000**, *39*, 806−809.

(37) Heinen, S.; Meyer, W.; Walder, L. Charge trapping in dendrimers with a viologen skeleton and a radial redox gradient. *J. Electroanal. Chem.* **2001**, *498*, 34−43.

(38) Mauritz, K. A.; Moore, R. B. State of Understanding of Nafion. *Chem. Rev.* **2004**, *104*, 4535−4585.

https://dx.doi.org/10.1021/acsaem.0c00067
ACS Appl. Energy Mater. XXXX, XXX, XXX−XXX